Chemistry & Biology
Article

# Free Glycine Accelerates the Autoproteolytic Activation of Human Asparaginase

Ying Su,[1] Christos S. Karamitros,[2] Julian Nomme,[1] Theresa McSorley,[2] Manfred Konrad,[2] and Arnon Lavie[1,*]
[1]Department of Biochemistry and Molecular Genetics, University of Illinois at Chicago, Chicago, IL 60607, USA
[2]Max Planck Institute for Biophysical Chemistry, 37077 Goettingen, Germany
*Correspondence: lavie@uic.edu
http://dx.doi.org/10.1016/j.chembiol.2013.03.006

## SUMMARY

**Human asparaginase 3 (hASNase3), which belongs to the N-terminal nucleophile hydrolase superfamily, is synthesized as a single polypeptide that is devoid of asparaginase activity. Intramolecular autoproteolytic processing releases the amino group of Thr168, a moiety required for catalyzing asparagine hydrolysis. Recombinant hASNase3 purifies as the uncleaved, asparaginase-inactive form and undergoes self-cleavage to the active form at a very slow rate. Here, we show that the free amino acid glycine selectively acts to accelerate hASNase3 cleavage both in vitro and in human cells. Other small amino acids such as alanine, serine, or the substrate asparagine are not capable of promoting autoproteolysis. Crystal structures of hASNase3 in complex with glycine in the uncleaved and cleaved enzyme states reveal the mechanism of glycine-accelerated posttranslational processing and explain why no other amino acid can substitute for glycine.**

## INTRODUCTION

The human genome codes for at least three enzymes capable of hydrolyzing the amino acid asparagine to aspartate and ammonia. The most-studied enzyme is the lysosomal aspartylglucosaminidase (AGA), whose function is to remove carbohydrate groups linked to asparagine, as the final step in the degradation of cell-surface glycoproteins (Oinonen et al., 1995). Defects in AGA are the cause of aspartylglucosaminuria, an inborn lysosomal storage disease (Saito et al., 2008). A second enzyme is called 60 kDa lysophospholipase, which has an N-terminal domain homologous to the *E. coli* type I asparaginase (Sugimoto et al., 1998). The third enzyme, and the focus of this work, is called L-asparaginase (also known as hASRGL1/ALP [Bush et al., 2002] or CRASH [Evtimova et al., 2004]). Due to the sequence and structural homology of this enzyme with the *E. coli* type III asparaginase, we refer to this human asparaginase as hASNase3. A member of the N-terminal nucleophile (Ntn) family of hydrolases (Brannigan et al., 1995), this 308 residue enzyme is produced as an inactive single polypeptide that must undergo a peptide-bond break between residues Gly167 and Thr168 to attain asparaginase activity. Cleavage releases the amino group of Thr168, and this endows the enzyme with catalytic activity. This mechanism of protease activation is different from that which occurs in proenzymes (zymogens) such as trypsinogen, pepsinogen, thrombin, or caspases, where the inactivating protein region is cleaved off, either through another protease or through autoproteolysis, and then separates from the now-active enzyme (Kassell and Kay, 1973; Wolan et al., 2009). Importantly, the fold of Ntn family members is unchanged after the cleavage reaction, with the N-terminal (referred to as the $\alpha$ chain) and C-terminal ($\beta$ chain) parts remaining tightly associated to build a single functional unit. The cleavage reaction of Ntn hydrolases occurs autocatalytically, without a need for proteases (Brannigan et al., 1995; Xu et al., 1999).

Expression of hASNase3 in normal human tissue, observed in all developmental stages except neonate (based on the expressed sequence tags database), is restricted to a few organs that include the testis, brain, esophagus, prostate, and proliferating endometrium (Bush et al., 2002; Weidle et al., 2009). Interestingly, it has also been detected in several human tumors (Weidle et al., 2009), but the implication or the role of hASNase3 in cancer biology is unknown. To increase our understanding of this enzyme, we recombinantly expressed hASNase3, which purified as the uncleaved form. Since the uncleaved enzyme is catalytically inactive, we sought conditions that would promote the transformation to the cleaved and active state. We report that the free amino acid glycine highly selectively acts to promote the autocleavage reaction of hASNase3 in a concentration-, temperature-, and time-dependent manner. In addition, we present crystal structures of hASNase3 in complex with glycine that provide a molecular basis for the glycine-induced autocleavage of the enzyme. We propose that glycine-dependent activation of hASNase3 is related to the altered metabolic profile of cells characterized by increased glycolysis and reduced flux through the tricarboxylic acid (TCA) cycle. Since de novo synthesis of aspartate requires the TCA cycle intermediate oxaloacetate, such cells can instead convert asparagine to aspartate using hASNase3. Glycine, synthesized from the glycolysis metabolite 3-phosphoglycerate via serine, would act as the sensor that regulates cellular aspartate concentrations via hASNas3 activation.

## RESULTS

### Correlation between Glycine and hASNase3 Cleavage

Upon bacterial expression and purification, hASNase3 exhibited a single ~40 kDa band on SDS-PAGE corresponding to the uncleaved form (Figure 1A). In contrast, when we purified the homologous *E. coli* type III asparaginase, the predominant form was the cleaved version that presents itself as two

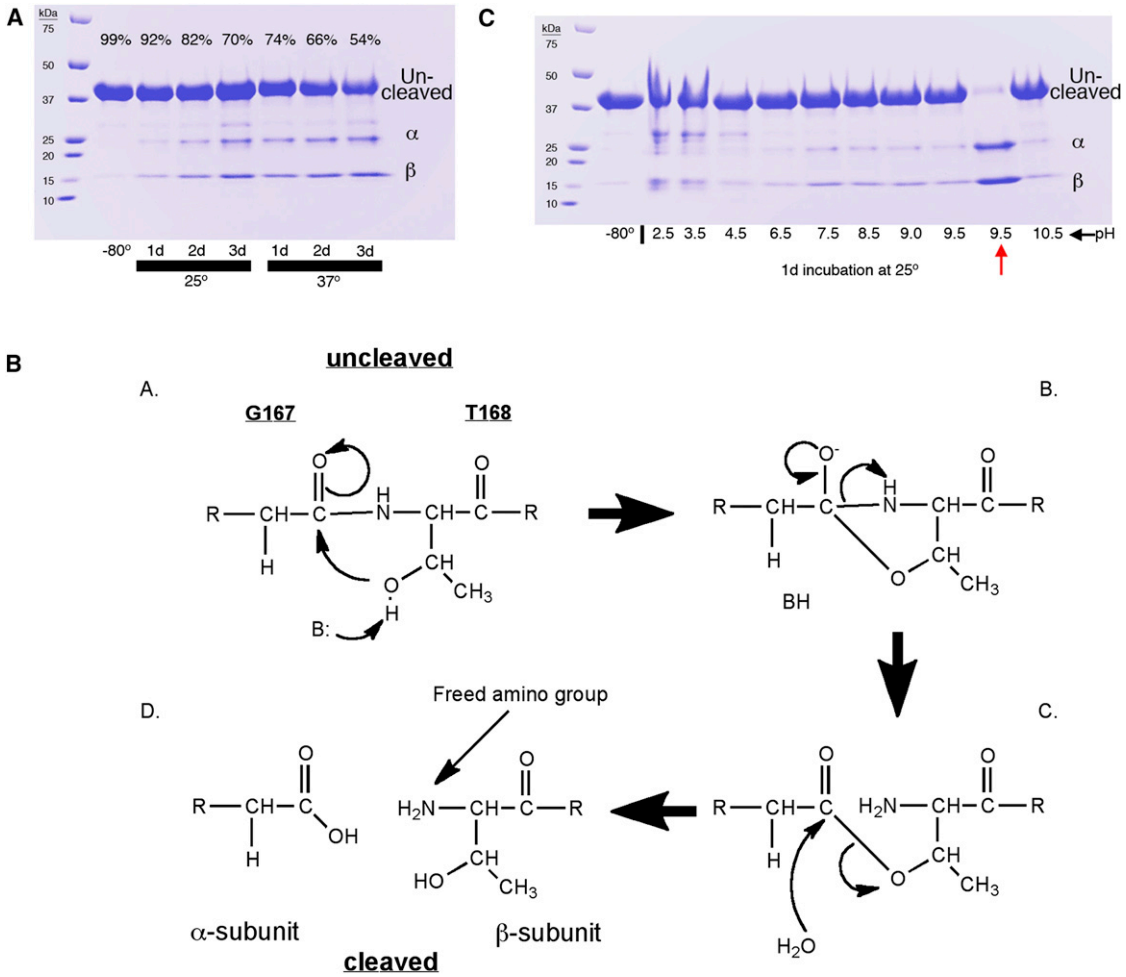


**Figure 1. Self-Cleavage of hASNase3 Is Slow in the Absence of Glycine**

(A) hASNase3 (4 mg/ml) was incubated in storage buffer at 25°C or 37°C, and samples were taken daily. Even after 3 days, the majority of the enzyme is still uncleaved (top band). Cleaved protein runs as two separate bands of lower molecular weight, representing the α and β subunits. Percentage denotes uncleaved band intensity relative to the sum of all forms (uncleaved + α + β).

(B) Schematic of the proposed cleavage reaction. A base (shown as B) would accept the proton from the hydroxyl group of Thr168. The identity of this base in the case of hASNase3 was not known prior to this work.

(C) hASNase3 was incubated for 1 day at 25°C at different pH values using appropriate buffers: citrate, pH 2.5–6.5; Tris, pH 7.5 and 8.5; Bicine, pH 9.0; TAPS, pH 9.5; glycine, pH 9.5 (red arrow); CAPS, pH 10.5. All buffers were at 100 mM. The enzyme sample prior to incubation is labeled −80°C in all figures.

See also Figures S1 and S2.

lower-molecular-weight bands on a gel (data not shown). The proportion of cleaved hASNase3 did increase gradually over time, but even after 3 days, the uncleaved form constituted ~70% of the protein incubated at 25°C and ~54% of the protein incubated at 37°C (Figure 1A; Figure S1 available online). The measured asparaginase activity of hASNase3 was proportional to the amount of cleaved enzyme, indicating that only the cleaved state was catalytically competent (data not shown). The extremely slow and incomplete self-cleavage of hASNase3 is consistent with a previous report (Cantor et al., 2009), but is different from observations made with bacterial (Borek and Jaskólski, 2000; Borek et al., 2004) and plant (Michalska et al., 2006) asparaginases, which showed efficient autoproteolysis in vitro even at 4°C, with the bacterial enzyme being fully cleaved in the first purification steps.

Analogy to other studied Ntn family members (Michalska et al., 2008) suggested that self-cleavage commences with the side chain of Thr168 acting as a nucleophile that attacks the carbonyl of Gly167 (Figure 1B, subpanel A). Note that the essential residue Thr168 of hASNase3 plays a dual role. First, its side chain is required for the cleavage reaction. Second, with the break of the peptide bond between Gly167 and Thr168, the freed amino group of Thr168 participates in catalyzing the hydrolysis of asparagine. A base that would accept the proton from the Thr168 hydroxyl group would accelerate the first step of the cleavage reaction. In several Ntn enzymes, the side chain of an aspartic acid residue prior to the scissile bond acts as this base (Qian et al., 2003), but in hASNAse3 the residue preceding Thr168 is a glycine. When replacing this glycine with aspartate in hASNase3, no cleavage was detected (data not shown).

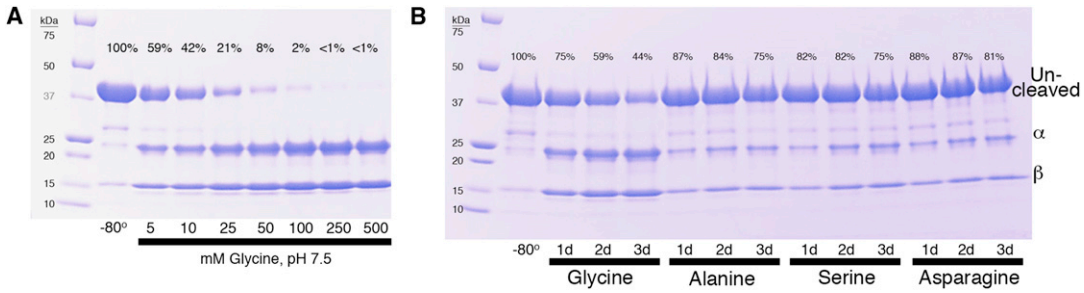


**Figure 2. Increase in Extent of hASNase3 Cleavage Is Specifically Dependent on Glycine**

(A) hASNase3 was incubated at 25°C for 42 hr in storage buffer containing increasing glycine concentrations at pH 7.5. There is a glycine-dose-dependent increase in the extent of cleavage. Percentage reflects quantification of uncleaved band intensity, with enzyme prior to incubation set at 100%.

(B) hASNase3 was incubated at 25°C in storage buffer supplemented with 10 mM glycine, alanine, serine, or asparagine, and samples were taken daily for 3 days. Quantification as in (A). In all conditions, the amount of cleaved hASNase3 slowly increases due to the intrinsic rate of autoproteolysis. However, only glycine accelerates autocleavage beyond the intrinsic rate.

See also Figures S3, S4, S8, and S9.

Interestingly, the *E. coli* type III enzyme, like the human enzyme, has a glycine residue preceding the cleavage site, yet it undergoes self-cleavage efficiently (Borek et al., 2004). This points to divergence in the mechanism of cleavage between Ntn family members. After building the tetrahedral intermediate, water is thought to act to complete the hydrolysis reaction (Figure 1B, subpanel C). Due to the observation of very slow cleavage of hASNase3 at physiological pH, we reasoned that a high pH would promote deprotonation of the Thr168 hydroxyl, making it more nucleophilic. However, incubation of hASNase3 in three different buffers spanning the pH range of 9 to 10 showed no increase in the cleaved form of the enzyme (Figure S2). When repeating the pH-scanning experiment in a wider pH range (from 2.5 to 10.5), all but one of the ten pH conditions tested showed the single band of the uncleaved enzyme, whereas at pH 9.5, using a glycine buffer, we observed essentially complete cleavage of hASNase3 (Figure 1C, red arrow). The two lower-molecular-weight bands of about 22 and 15 kDa observed with glycine buffer correspond to residues 1–167 (α chain) and 168–308 (β-chain), respectively, of the cleaved enzyme. This finding was surprising since we had already tested this pH range and saw no increase in cleavage (Figure S2). Indeed, the lane adjacent to the glycine-treated sample (Figure 1C) contained TAPS buffer at the same pH of 9.5, yet showed very little cleavage. This suggested that glycine, rather than simply the pH, must play a critical role in promoting cleavage of hASNase3, potentially as the base depicted in Figure 1B.

Next, we assessed the dependence of self-cleavage on the glycine concentration and pH. Indeed, the extent of cleavage was glycine-dose dependent (Figure 2A), and even the lowest glycine concentration (5 mM) promoted 40% cleavage, a cleavage amount requiring ~11 days in a buffer lacking glycine (Figure S1). Significantly, this glycine acceleration of hASNase3 cleavage occurs at the physiological pH of 7.5 nearly as efficiently as at pH 9.5 (Figure S3). We wondered whether other amino acids could function as cleavage accelerators. Since this would presumably require the binding of the amino acid to the active site of hASNase3, we reasoned that amino acids with small side chains would have a greater chance of replacing glycine. However, the addition of alanine or serine did not increase the proportion of cleaved enzyme above that obtained by intrinsic cleavage (Figure 2B). Moreover, the substrate asparagine also did not accelerate the cleavage rate beyond its intrinsic rate. Likewise, small-molecule metabolites, such as glycolate, glyoxylate, sarcosine, oxalate, choline, or ethanolamine, failed to trigger or inhibit the cleavage reaction (Figure S4).

We also examined the effects of these metabolites on the asparaginase activity of the cleaved enzyme. Indeed, the cleavage-activator glycine, as well as some of these compounds at relatively high concentration, inhibited the activated form of the enzyme. While glycine at either 10 or 50 mM reduced asparaginase activity by about 50%, glycolate, glyoxylate, oxalate, L-aspartate, and serine showed a concentration-dependent effect, lowering the catalytic activity by up to 5-fold at nonphysiological 50 mM (Figure S5). This demonstrates that several of the tested compounds have the ability to bind to the enzyme (at least to the cleaved form), but only glycine has the ability to promote the cleavage reaction.

## Structural Analysis of hASNase3

To understand the mechanism behind the glycine-induced cleavage reaction, we solved the crystal structure of uncleaved hASNase3 in complex with glycine. Our previous work on hASNase3 (Nomme et al., 2012) revealed that, depending on the age of our crystals, we can obtain the structure of either the uncleaved (using fresh crystals) or cleaved state (using crystals grown several months earlier). In those structures, we observed a precipitant molecule (e.g., malonate, sulfate) occupying the asparagine-binding site. In fact, due to competition between the precipitant and any added amino acid, in order to obtain the hASNase3-ASP complex, we had to transfer the crystals out of the precipitant and into a highly concentrated ASP solution (Nomme et al., 2012). Based on this experience, to obtain the uncleaved hASNase3-glycine complex, we used freshly prepared crystals, which were transferred to a 3 M glycine solution. The high glycine concentration was required to stabilize the crystal in the absence of the precipitant and to supply the glycine for complex formation. Despite using fresh crystals that were exposed only shortly to a pH 7.5 glycine solution, diffraction data revealed full hASNase3 cleavage. Based on the cleavage

**Table 1. Data Collection and Refinement Statistics**

| Complex | GLY, pH 4.9 | GLY, pH 3.3 |
|---|---|---|
| Protein Data Bank codes | 4HLP | 4HLO |
| X-ray source and detector | SERCAT BM | SERCAT ID |
| | MARCCD 225 | MARCCD 300 |
| Wavelength (Å) | 1.0 | 1.0 |
| Temperature (K) | 100 | 100 |
| Resolution[a] (Å) | 1.91 (1.91–2.02) | 1.95 (1.95–2.0) |
| Number of reflections | | |
| Observed | 144,084 | 425,284 |
| Unique | 45,006 | 43,500 |
| Completeness (%) | 95.7 (81.7) | 98.2 (90.0) |
| $R_{sym}$ (%) | 5.5 (37.9) | 12.5 (51.2) |
| I/σ(I) | 12.40 (1.55) | 12.70 (2.12) |
| Space group | P $6_5$ | P $6_5$ |
| Unit cell (Å) | | |
| a = b | 59.74 | 59.94 |
| c | 301.53 | 301.10 |
| Refinement program | REFMAC5 | REFMAC5 |
| Twinning fraction | 0.514 | 0.505 |
| Refinement statistics | | |
| $R_{cryst}$ (%) | 18.4 | 16.7 |
| $R_{free}$ (%) | 22.4 | 20.9 |
| Resolution range (Å) | 30 - 1.91 | 30 - 1.95 |
| Protein molecules per a.u. | 2 | 2 |
| Number of atoms | | |
| Protein | 2,158, 2,158 | 2,196, 2,199 |
| Glycine | 5 × 4 | 5 × 5 |
| Water | 181 | 176 |
| Rmsd | | |
| Bond length (Å) | 0.009 | 0.011 |
| Bond angles (°) | 1.116 | 1.354 |
| Average B-factors (Å$^2$) /chain | | |
| Protein | 31, 32 | 24, 24 |
| Glycine | 34 | 33 |
| Water molecules | 32 | 23 |
| Ramachandran plot | | |
| Most favored regions (%) | 92.2 | 88.5 |
| Additionally allowed regions (%) | 7.2 | 10.5 |
| Generously allowed regions (%) | 0.2 | 0.6 |
| Disallowed regions (%) | 0.4 | 0.4 |

[a]Last shell in parentheses.

mechanism (Figure 1B), we reasoned that a lower pH and an even shorter soak time would allow us to trap the enzyme in its precleaved state, the state relevant for probing the glycine-induced cleavage reaction. Yet again, a data set (1.91 Å resolution; Table 1) collected from a crystal soaked in 3 M glycine (pH 4.9) for <1 min showed full protein cleavage (Figure 3A). In this postcleavage state of hASNase3, glycine bound at the active site very similarly to the product aspartate (Nomme et al., 2012), forming interactions with the conserved residues Arg196 via its carboxylic acid moiety and Asp199 via its amino group (Figure 3B). The sole interaction with Thr168 occurs between the glycine amino group and the hydroxyl moiety of Thr168 (3.3 Å). This glycine-binding mode failed to clarify how the amino acid would act to accelerate peptide cleavage between Gly167 and Thr168.

The observation of a fully cleaved enzyme state in the pH 4.9 soaked crystal prompted us to test an even lower pH. Indeed, by soaking a crystal of hASNase3 in a glycine solution of pH 3.3, we successfully obtained the complex in the precleaved enzyme state (Figure 3C). For the uncleaved enzyme, we could model the entire polypeptide chain except four residues that span Gln158 and Gln163. The electron density of the scissile bond between Gly167 and Thr168 clearly shows an intact peptide bond (Figure 3D). In this complex structure, solved at 1.95 Å resolution, we again observed the previously mentioned glycine molecule at the substrate-binding site, making very similar interactions as noted in the pH 4.9 structure (labeled GLY1 in Figure 3C). Unexpectedly, an additional glycine molecule occupied the active site (labeled GLY2 in Figures 3C and S6), this time spanning the conserved threonines at positions 168 and 219. Notably, the carboxylic acid group of this second glycine is at only 2.6 Å distance to the hydroxyl of the catalytically essential Thr168. This type of interaction would allow GLY2 to act as the base that accepts the proton from the Thr168 hydroxyl group, thereby activating it to attack the carbonyl group of the preceding residue, Gly167. We analyzed the binding site of GLY2 in the hASNase3 active site in order to understand why no other amino acid could substitute for glycine in promoting cleavage (Figure 2B). Modeling of alanine in place of GLY2 reveals a steric clash between the methyl side-chain and main-chain atoms of hASNase3 (Figure S7). This rationalizes why even the next-smallest amino acid, alanine, would be sterically excluded from the GLY2 binding site, and hence the cleavage-promoting specificity of glycine. It is of interest to mention here that the dipeptide glycylglycine does not induce (Figure S4) or inhibit autocleavage (Figure S8) or affect the asparaginase activity of the activated enzyme (Figure S5), suggesting that glycylglycine lacks the ability to bind to the hASNas3 active site.

## Glycine Promotes hASNase3 Cleavage in Human Cells

We next asked whether glycine-accelerated cleavage, and hence activation, also occurs in mammalian cells. HEK293 cells were transiently transfected with the hASNase3 gene, and hASNase3 expression level and molecular state were monitored using western blot analysis (Figure 4). Cells grown in regular media, without glycine supplementation, predominantly expressed uncleaved hASNase3 (Figure 4). Note that the media used for the cell culture experiments contained 135 μM glycine, not taking into account any glycine coming from the fetal bovine serum. This explains the low, but not absent, cleavage of hASNase3 in this condition. The addition of an extra 1 mM glycine to the media resulted in a more than 25% reduction of uncleaved protein with a concomitant increase in the cleaved forms. Higher concentrations of glycine promoted progressively increased protein cleavage, such that at 5 mM added glycine, less than 10% remains in the uncleaved state, with approximately complete cleavage occurring at higher glycine concentrations after the same incubation time.

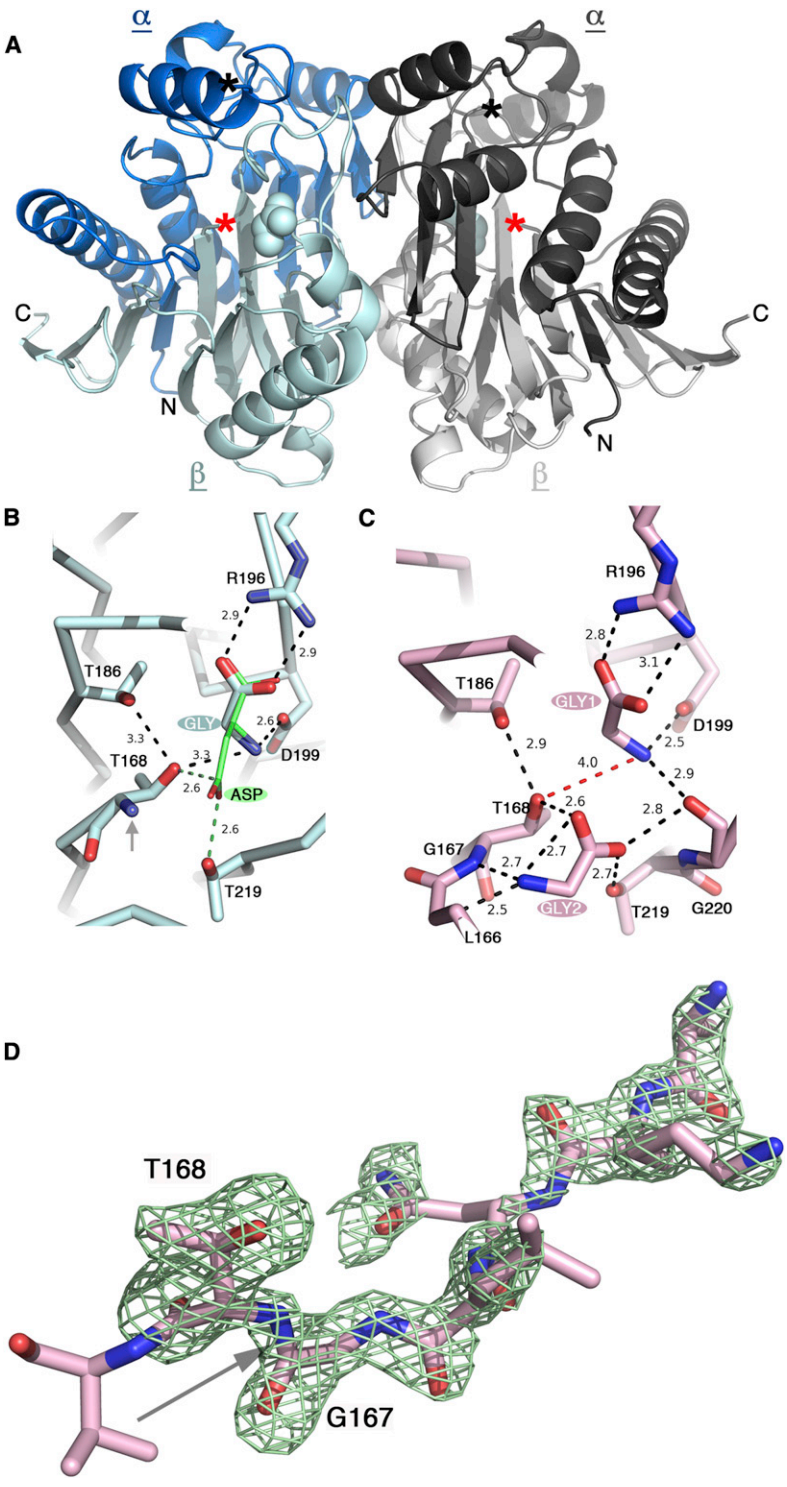


**Figure 3. hASNase3 Structure in Complex with Glycine**

(A) The cleaved state of the homodimeric enzyme, obtained from crystals soaked in a 3 M glycine solution, pH 4.9, is depicted. One protomer is colored in dark and light blue, and the other in dark and light gray. The dark and light shades depict the α and β chains, respectively. The glycine bound at the active site is depicted as a space-filling object. The black star denotes the most C-terminal residue of the α chain with traceable electron density, and the red star denotes the N-terminal residue of the β chain, which is Thr168.

(B) Active-site residues in the cleaved hASNase3-GLY complex structure at pH 4.9. Gray arrow denotes the free amino group of Thr168 resulting from cleavage. Glycine binds in a similar fashion to aspartate (green; as seen in the hASNase3-ASP complex structure; Protein Data Bank code 4GDW). Distances are in angstroms.

(C) The uncleaved hASNase3-GLY complex structure at pH 3.3. Two free glycine molecules are present at the active site. Glycine 1 (GLY1) binds in the same position as the glycine in (B), and glycine 2 (GLY2) binds in proximity to the scissile bond. Importantly, GLY2 interacts directly with the Thr168 OH group via its carboxylic acid moiety (2.6 Å). It is this interaction that can serve to activate Thr168 to attack the carbonyl group of Gly167.

(D) The Fo-Fc omit map contoured at the 3 sigma level displays the uncleaved peptide bond. To avoid model bias, residues 163 to 168 were omitted from the model, which then underwent multiple refinement rounds. The difference electron density map reveals the conformation of Thr168 and of the residues that precede it. This region, despite being uncleaved, seems to have increased mobility relative to the core structure. As a result, some side-chain densities (e.g., Leu166, Asn165) are not contiguous but clearly present. The increased mobility of this region was also observed in the structures of hASNase3 mutants that cannot undergo cleavage (data not shown). A gray arrow points to the peptide bond that breaks as hASNase3 is cleaved into the α and β chains.

See also Figures S6 and S7.

## DISCUSSION

Here, we report that physiologically relevant glycine concentrations can dramatically accelerate, and drive to completion, the weak intrinsic self-cleavage reaction of hASNase3. While we do find that millimolar glycine levels are required for efficient cleavage (Figure 4), concentrations between 3 and 8 mM (depending on the tissue examined) have been measured in vivo (Pitkänen et al., 2003). Remarkably, the most recent work, which examined the role of the pyruvate kinase isoform M2 (PKM2) in regulating glycolytic flux in cancer cells and the dependence of PKM2 activity on serine and glycine biosynthesis, revealed intracellular accumulation of free glycine of up to 10 mM (Chaneton et al., 2012), a concentration that would promote complete cleavage of hASNase3 (Figure 4). Glycine did not activate PKM2 in cells or in vitro, yet this work demonstrated serine as the only amino acid to do so in vitro, with this finding being further substantiated by structural analyses of PKM2-serine complexes (Chaneton et al., 2012). In the case of hASNase3, we discovered a specific role of glycine in activating the enzyme both in vitro and in cells. This prompts the following questions: What is the relevance of glycine levels in cells to hASNase3's in vivo function, specifically to any potential role of glycine as a regulator of hASNase3 activity? Can we rationalize its expression pattern in normal tissue and in several

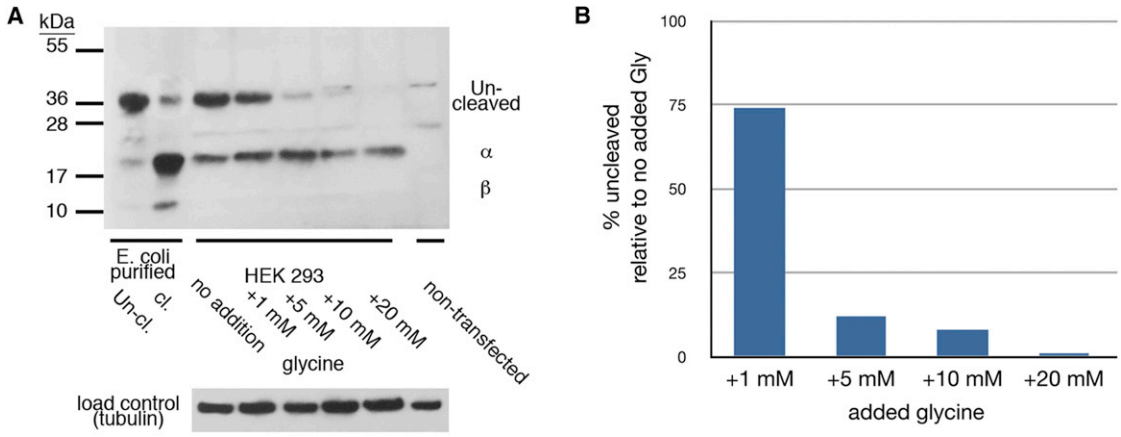


**Figure 4. Glycine Promotes hASNase3 Cleavage in Human Cells**

(A) Western blot of HEK293 cells transfected with the gene for hASNase3, grown in regular media or in media supplemented with the noted glycine levels for 2 days. Detection of the hASNase3 state was done using polyclonal antibodies raised against the full-length protein. Antibodies detect well the uncleaved enzyme and the α subunit, but give only a weak signal for the β subunit. The uncleaved (Un-cl) and cleaved (cl) human enzyme purified from *E. coli* is shown for reference. Protein loading control is shown below.

(B) Quantification of the uncleaved band, with the condition of no glycine supplementation set at 100%.

human tumors? We note that hASNase3 has dual asparaginase and isoaspartyl peptidase activities (isoaspartyl peptide linkages are a common source of protein damage; Aswad et al., 2000), with seemingly similar kinetic efficiencies (Cantor et al., 2009). This causes ambiguity as to the precise physiological function of hASNase3. In this context, it is worth recalling that human AGA also has dual catalytic function, hydrolyzing β-aspartyl-glucosamine linkages in glycoproteins and various β-aspartyl-amides, including asparagine itself. Moreover, the threonine aspartase Taspase1 acts as an endopeptidase that cleaves the mixed-lineage leukemia protein (Hsieh et al., 2003), the basal transcription factor TFIIA (Hsieh et al., 2003), and other intracellular substrates after an aspartate residue in the recognition sequence (Bier et al., 2011). Like hASNase3, these enzymes belong to the Ntn-hydrolase protein family where the full-length enzymes undergo posttranslational autoproteolytic processing, liberating the N-terminal threonine of the β subunit as the catalytic nucleophile. This threonine residue has been shown by mutational analyses to act as the nucleophile for both autoproteolysis and hydrolase activity. While several residues critical for self-cleavage have been identified in human AGA (Bier et al., 2011), no regulatory, or triggering, factor is known for this intramolecular activation step. In contrast, in the case of hASNase3, our work reveals that free glycine very selectively triggers this activation process, which suggests a link to physiological situations of increased glycine levels.

In the physiological context, one intriguing possibility relates to situations where intracellular glycine levels are increased with a concomitant decrease in aspartate levels. This metabolic imbalance is observed in cancer cells where altered gene expression increases the flux through glycolysis (Warburg, 1956). One enzyme implicated in increased glycolysis is PKM2, which is detected in cancer cells and replaces the catalytically more efficient M1 isoform (Vander Heiden et al., 2009). The consequence of reduced pyruvate kinase activity is closure of the spigot connecting the glycolytic pathway to the TCA cycle. This allows for the diversion of glycolysis intermediates for the synthesis of essential metabolites. In fact, it was recently shown that a small-molecule activator of PKM2 induces serine auxotrophy, an amino acid whose synthesis relies on the glycolytic intermediate 3-phosphoglycerate (Kung et al., 2012). A second enzyme involved in diverting glycolytic intermediates into serine biosynthesis is phosphoglycerate dehydrogenase, and this activity has also been proposed to contribute to cancer cell proliferation (Locasale et al., 2011). As glycine is generated from serine, increased glycolytic flux would increase the glycine levels, as demonstrated by studies of a cancer cell line (Locasale et al., 2011) and brain tumors in vivo (Maher et al., 2012). A recent metabolite-profiling study of NCI-60 cancer cell lines correlated glycine levels with proliferation rates, showcasing the important role of this amino acid in rapidly dividing cells (Jain et al., 2012).

At the same time, increased glycolytic flux reduces the flow of metabolites to the TCA cycle. Reduced TCA flux limits the synthesis of molecules that originate from TCA intermediates. One specific example of such a molecule is the amino acid aspartate, whose de novo synthesis requires the TCA intermediate oxaloacetate. Indeed, a marked decrease in the level of the amino acid aspartate was observed in rat brain gliomas (Ziegler et al., 2001). The data we present here suggest that one mechanism used by cells to counter low TCA flux is to activate the enzyme hASNase3, which then provides the required aspartic acid by catalyzing asparagine hydrolysis. Thus, activation of hASNase3 by glycine would compensate for the lack of aspartate by converting asparagine to aspartate.

Thus, we suggest a model where cancer cells usurp a regulatory mechanism (i.e., dependency of hASNase3 activation on glycine levels) that pre-exists in noncancer cells (see below) that normally express hASNase3 for the purpose of maintaining the required metabolic balance. This model, which relates the activity of metabolic enzymes to metabolite levels in order to compensate for the altered metabolic requirements of rapidly dividing cells, implies that inhibitors of such enzymes (e.g.,

hASNase3) could be explored as potential cancer therapeutics. In fact, the targeting of enzymes that supply asparagine, in order to limit cancer cell proliferation, is currently being explored by inhibiting asparagine synthetase (Richards and Kilberg, 2006). We examined additional metabolites other than glycine that are increased in glycolytic cells, such as pyruvate and lactate, but these failed to recapitulate glycine's ability to accelerate hASNase3 cleavage (Figure S9), highlighting the glycine specificity of this process.

Finally, the cancer implications of hASNase3 raise questions on its role in normal cells and the properties of these normal cells vis-à-vis glycine and aspartate concentrations. Consistent with our model, it has been reported that normal brain (Coles et al., 2000) and testis (Liu et al., 2011), two organs with high hASNase3 expression, have increased glycolytic activity. Additionally, protein analyses of sperm extracts (Bush et al., 2002) revealed hASNase3 in the predominately cleaved form, thereby correlating the cleaved state of the enzyme with high glycine levels. Further studies that probe the levels of amino acids in normal and diseased states, and the cellular response to these changes, are warranted.

## SIGNIFICANCE

**Human asparaginase 3 is an Ntn-family hydrolase requiring cleavage between Gly167 and Thr168 for enzymatic activity. Autoproteolysis of recombinantly produced hASNase3 is very slow. We discovered that the free amino acid glycine dramatically increases the rate and extent of cleavage. Other amino acids or various small-molecule metabolites tested in vitro are not capable of promoting self-cleavage. The crystal structure of uncleaved hASNase3 in complex with glycine explains the ability of the amino acid to promote this intramolecular reaction. We observe two glycine molecules bound at the active site. The first binds at the same position as the substrate asparagine. The second glycine is positioned such that its carboxylic acid moiety is in close proximity to the Thr168 hydroxyl group. The latter binding mode would allow glycine to act as a base that activates the hydroxyl group to attack the carbonyl group of the preceding Gly167, thereby initiating the cleavage reaction. The enzyme has limited expression in normal tissue, being confined mainly to the testis and brain. Notably, it has also been detected in several cancers. A unifying feature of tissues that express hASNase3 is high glycolytic level. Increased flux through glycolysis would promote glycine synthesis, as it is generated from the glycolysis metabolite 3-phosphoglycerate via serine. At the same time, aspartate levels would be decreased, as de novo synthesis of this amino acid requires the TCA cycle intermediate oxaloacetate. Together, this implies that the function of hASNase3 is to increase the level of aspartate as compensation for its reduced synthesis and that the enzyme's activity is regulated by the glycine concentration. The requirement of highly glycolytic cells, such as those found in cancers, to generate sufficient levels of key metabolites, such as aspartate, suggests that molecules inhibiting hASNase3 may act to reduce cancer cell proliferation.**

## EXPERIMENTAL PROCEDURES

### Cloning, Expression, and Purification of Human ASNase3

The cloning and expression of hASNase3 have been reported previously (Nomme et al., 2012). In short, *E. coli* BL21(DE3) C41 carrying a modified pET14b to include a SUMO tag was grown at 37°C. Upon reaching an optical density of 0.6–0.8, the temperature was reduced to 18°C and 0.5 mM IPTG was added to induce expression. After cell lysis by sonication, the enzyme was purified using a metal affinity column and the SUMO tag was cleaved by SUMO protease, followed by gel filtration. The fractions containing hASNse3 were concentrated to 38 mg/ml, aliquoted, and stored at −80°C.

### Crystallization of hASNase3

A total of 1 μl of hASNase3 at 38 mg/ml (in 25 mM Tris [pH 7.5], 200 mM NaCl, 2 mM DTT) was mixed with 1 μl of the reservoir solution (2.2 M sodium malonate) on a glass coverslip and left to undergo vapor diffusion using the hanging drop method at 20°C. To form the glycine complex, a crystal was transferred to a 3 M glycine, pH 7.5 solution. Diffraction data on this crystal revealed the cleaved state of the enzyme and a glycine molecule at the active site. To obtain a complex with the uncleaved enzyme, glycine solutions of lower pH were tested. At pH 4.9, crystals of the cleaved form were obtained (identical to those soaked at pH 7.5). However, soaking at pH 3.3 yielded crystals with the uncleaved protein.

### Data Collection and Structure Solution of hASNase3

Diffraction data were collected at the Advanced Photon Source (APS) located at Argonne National Laboratory, using the SERCAT beamlines (see Table 1 for data collection and refinement statistics). The structures were refined with Refmac5 (Murshudov et al., 1997). All crystals were perfectly twinned, with the true space group being $P6_5$ (apparent space group, $P6_522$) and contained two copies of hASNase3 (that is, an αβ dimer) in the asymmetric unit. Refinement using the twin option in Refmac5 showed a twin domain fraction of ~50%. Data collected for freshly grown crystals showed the uncleaved state of the enzyme, whereas in older crystals the enzyme was in the cleaved state. Attempts to soak in the product aspartate (ASP) or glycine (GLY), even at a concentration of 100 mM, failed to reveal electron density for these amino acids. We interpret this as being due to competition by the precipitant salt. To obtain the GLY complex, we transferred the crystals to a 3 M glycine solution. The rationale was that a high concentration of glycine would act as a precipitant to keep the crystals stable (attempts to transfer the crystals to a nonsalt condition such as PEG were unsuccessful) and would also supply the GLY molecule bound at the active site. Diffraction data collected on a crystal soaked in 3 M GLY pH 7.5 revealed the fully cleaved state (data not shown). The same result was obtained with a crystal soaked in 3 M GLY, pH 4.9. In contrast, we observed the uncleaved state in a crystal soaked in 3 M GLY, pH 3.3.

For the cleaved pH 4.9 hASNase3-GLY complex (described here), we could model residues 1 to 153 of the α chain (no traceable density for residues 154–167) and 168–308 of the β chain. For the uncleaved pH 3.3 GLY complex, we could model all residues except 158–163. The electron density for the residues immediately preceding the cleavage site was unambiguous (Figure 3D). All structure figures were made with PyMol.

### Western Blot Experiments

HEK293 cells, grown in RPMI 1640 supplemented with 10% fetal bovine serum, were transfected to express hASNase3, and cell lysates were analyzed by western blots. All SDS-PAGE gel band intensities were quantified using ImageJ. Polyclonal antibodies against hASNase3 were generated by immunizing rabbits with 0.6 mg of SDS-PAGE-purified full-length protein according to the Eurogentec (Seraing, Belgium) custom antibody production protocol. For expressing and analyzing the enzyme in a human cell line, the gene coding for hASNase3 was transferred from the pET14b vector to a pcDNA3.1(−) (Invitrogen) with the addition of a Kozak sequence. HEK293 cells ($3 \times 10^6$) were grown to 90%–95% confluency and then transfected using Lipofectamine 2000 (Invitrogen). At this point, glycine at various concentrations was added to the media. Cells were then incubated at 37°C with 5% $CO_2$. After 2 days, cells were harvested and lysates analyzed by western blots. Loading controls were done using a tubulin antibody.

## ACCESSION NUMBERS

The structures of hASNase3 have been deposited in the Protein Data Bank under accession codes 4HLP (GLY pH 4.9) and 4HLO (GLY pH 3.3).

## SUPPLEMENTAL INFORMATION

Supplemental Information includes nine figures and can be found with this article online at http://dx.doi.org/10.1016/j.chembiol.2013.03.006.

## ACKNOWLEDGMENTS

We thank A. Mankin for his comments on the manuscript, J. Kaplan and M. Caffrey for discussions, U. Welscher-Altschäffel for technical assistance, and C. Gemski for editing advice. Diffraction data were collected at Southeast Regional Collaborative Access Team beamlines at the Advanced Photon Source, Argonne National Laboratory. Use of the Advanced Photon Source was supported by the US Department of Energy, Office of Science, Office of Basic Energy Sciences, under contract no. W-31-109-Eng-38. This work was supported by National Institutes of Health grant R21 CA155424, the Max Planck Society, and the Deutsche Forschungsgemeinschaft (to T.M.).

Received: October 18, 2012
Revised: February 25, 2013
Accepted: March 4, 2013
Published: April 18, 2013

## REFERENCES

Aswad, D.W., Paranandi, M.V., and Schurter, B.T. (2000). Isoaspartate in peptides and proteins: formation, significance, and analysis. J. Pharm. Biomed. Anal. *21*, 1129–1136.

Bier, C., Knauer, S.K., Klapthor, A., Schweitzer, A., Rekik, A., Krämer, O.H., Marschalek, R., and Stauber, R.H. (2011). Cell-based analysis of structure-function activity of threonine aspartase 1. J. Biol. Chem. *286*, 3007–3017.

Borek, D., and Jaskólski, M. (2000). Crystallization and preliminary crystallographic studies of a new L-asparaginase encoded by the Escherichia coli genome. Acta Crystallogr. D Biol. Crystallogr. *56*, 1505–1507.

Borek, D., Michalska, K., Brzezinski, K., Kisiel, A., Podkowinski, J., Bonthron, D.T., Krowarsch, D., Otlewski, J., and Jaskolski, M. (2004). Expression, purification and catalytic activity of Lupinus luteus asparagine beta-amidohydrolase and its Escherichia coli homolog. Eur. J. Biochem. *271*, 3215–3226.

Brannigan, J.A., Dodson, G., Duggleby, H.J., Moody, P.C., Smith, J.L., Tomchick, D.R., and Murzin, A.G. (1995). A protein catalytic framework with an N-terminal nucleophile is capable of self-activation. Nature *378*, 416–419.

Bush, L.A., Herr, J.C., Wolkowicz, M., Sherman, N.E., Shore, A., and Flickinger, C.J. (2002). A novel asparaginase-like protein is a sperm autoantigen in rats. Mol. Reprod. Dev. *62*, 233–247.

Cantor, J.R., Stone, E.M., Chantranupong, L., and Georgiou, G. (2009). The human asparaginase-like protein 1 hASRGL1 is an Ntn hydrolase with beta-aspartyl peptidase activity. Biochemistry *48*, 11026–11031.

Chaneton, B., Hillmann, P., Zheng, L., Martin, A.C., Maddocks, O.D., Chokkathukalam, A., Coyle, J.E., Jankevics, A., Holding, F.P., Vousden, K.H., et al. (2012). Serine is a natural ligand and allosteric activator of pyruvate kinase M2. Nature *491*, 458–462.

Coles, J.A., Véga, C., and Marcaggi, P. (2000). Metabolic trafficking between cells in nervous tissue. Prog. Brain Res. *125*, 241–254.

Evtimova, V., Zeillinger, R., Kaul, S., and Weidle, U.H. (2004). Identification of CRASH, a gene deregulated in gynecological tumors. Int. J. Oncol. *24*, 33–41.

Hsieh, J.J., Cheng, E.H., and Korsmeyer, S.J. (2003). Taspase1: a threonine aspartase required for cleavage of MLL and proper HOX gene expression. Cell *115*, 293–303.

Jain, M., Nilsson, R., Sharma, S., Madhusudhan, N., Kitami, T., Souza, A.L., Kafri, R., Kirschner, M.W., Clish, C.B., and Mootha, V.K. (2012). Metabolite profiling identifies a key role for glycine in rapid cancer cell proliferation. Science *336*, 1040–1044.

Kassell, B., and Kay, J. (1973). Zymogens of proteolytic enzymes. Science *180*, 1022–1027.

Kung, C., Hixon, J., Choe, S., Marks, K., Gross, S., Murphy, E., DeLaBarre, B., Cianchetta, G., Sethumadhavan, S., Wang, X., et al. (2012). Small molecule activation of PKM2 in cancer cells induces serine auxotrophy. Chem. Biol. *19*, 1187–1198.

Liu, F., Jin, S., Li, N., Liu, X., Wang, H., and Li, J. (2011). Comparative and functional analysis of testis-specific genes. Biol. Pharm. Bull. *34*, 28–35.

Locasale, J.W., Grassian, A.R., Melman, T., Lyssiotis, C.A., Mattaini, K.R., Bass, A.J., Heffron, G., Metallo, C.M., Muranen, T., Sharfi, H., et al. (2011). Phosphoglycerate dehydrogenase diverts glycolytic flux and contributes to oncogenesis. Nat. Genet. *43*, 869–874.

Maher, E.A., Marin-Valencia, I., Bachoo, R.M., Mashimo, T., Raisanen, J., Hatanpaa, K.J., Jindal, A., Jeffrey, F.M., Choi, C., Madden, C., et al. (2012). Metabolism of [U-13 C]glucose in human brain tumors in vivo. NMR Biomed. *25*, 1234–1244.

Michalska, K., Bujacz, G., and Jaskolski, M. (2006). Crystal structure of plant asparaginase. J. Mol. Biol. *360*, 105–116.

Michalska, K., Hernandez-Santoyo, A., and Jaskolski, M. (2008). The mechanism of autocatalytic activation of plant-type L-asparaginases. J. Biol. Chem. *283*, 13388–13397.

Murshudov, G.N., Vagin, A.A., and Dodson, E.J. (1997). Refinement of macromolecular structures by the maximum-likelihood method. Acta Crystallogr. D Biol. Crystallogr. *53*, 240–255.

Nomme, J., Su, Y., Konrad, M., and Lavie, A. (2012). Structures of apo and product-bound human L-asparaginase: insights into the mechanism of autoproteolysis and substrate hydrolysis. Biochemistry *51*, 6816–6826.

Oinonen, C., Tikkanen, R., Rouvinen, J., and Peltonen, L. (1995). Three-dimensional structure of human lysosomal aspartylglucosaminidase. Nat. Struct. Biol. *2*, 1102–1108.

Pitkänen, H.T., Oja, S.S., Kemppainen, K., Seppä, J.M., and Mero, A.A. (2003). Serum amino acid concentrations in aging men and women. Amino Acids *24*, 413–421.

Qian, X., Guan, C., and Guo, H.C. (2003). A dual role for an aspartic acid in glycosylasparaginase autoproteolysis. Structure *11*, 997–1003.

Richards, N.G., and Kilberg, M.S. (2006). Asparagine synthetase chemotherapy. Annu. Rev. Biochem. *75*, 629–654.

Saito, S., Ohno, K., Sugawara, K., Suzuki, T., Togawa, T., and Sakuraba, H. (2008). Structural basis of aspartylglucosaminuria. Biochem. Biophys. Res. Commun. *377*, 1168–1172.

Sugimoto, H., Odani, S., and Yamashita, S. (1998). Cloning and expression of cDNA encoding rat liver 60-kDa lysophospholipase containing an asparaginase-like region and ankyrin repeat. J. Biol. Chem. *273*, 12536–12542.

Vander Heiden, M.G., Cantley, L.C., and Thompson, C.B. (2009). Understanding the Warburg effect: the metabolic requirements of cell proliferation. Science *324*, 1029–1033.

Warburg, O. (1956). On the origin of cancer cells. Science *123*, 309–314.

Weidle, U.H., Evtimova, V., Alberti, S., Guerra, E., Fersis, N., and Kaul, S. (2009). Cell growth stimulation by CRASH, an asparaginase-like protein overexpressed in human tumors and metastatic breast cancers. Anticancer Res. *29*, 951–963.

Wolan, D.W., Zorn, J.A., Gray, D.C., and Wells, J.A. (2009). Small-molecule activators of a proenzyme. Science *326*, 853–858.

Xu, Q., Buckley, D., Guan, C., and Guo, H.C. (1999). Structural insights into the mechanism of intramolecular proteolysis. Cell *98*, 651–661.

Ziegler, A., von Kienlin, M., Décorps, M., and Rémy, C. (2001). High glycolytic activity in rat glioma demonstrated in vivo by correlation peak 1H magnetic resonance imaging. Cancer Res. *61*, 5595–5600.

 